



SCHOOL of
GRADUATE STUDIES
EAST TENNESSEE STATE UNIVERSITY

East Tennessee State University
Digital Commons @ East
Tennessee State University

Electronic Theses and Dissertations

Student Works

12-2018

A Normal Form for Words in the Temperley-Lieb Algebra and the Artin Braid Group on Three Strands

Jack Hartsell

East Tennessee State University

Follow this and additional works at: <https://dc.etsu.edu/etd>

 Part of the [Applied Mathematics Commons](#)

Recommended Citation

Hartsell, Jack, "A Normal Form for Words in the Temperley-Lieb Algebra and the Artin Braid Group on Three Strands" (2018). *Electronic Theses and Dissertations*. Paper 3504. <https://dc.etsu.edu/etd/3504>

This Thesis - Open Access is brought to you for free and open access by the Student Works at Digital Commons @ East Tennessee State University. It has been accepted for inclusion in Electronic Theses and Dissertations by an authorized administrator of Digital Commons @ East Tennessee State University. For more information, please contact digilib@etsu.edu.

A Normal Form for Words in the Temperley-Lieb Algebra and the Artin Braid
Group on Three Strands

A thesis

presented to

the faculty of the Department of Mathematics

East Tennessee State University

In partial fulfillment

of the requirements for the degree

Master of Science in Mathematical Sciences

by

Jack Hartsell

December 2018

Frederick Norwood, Ph.D., Chair

Robert Gardner, Ph.D.

Rodney Keaton, Ph.D.

Keywords: knot theory, algebra, topology.

ABSTRACT

A Normal Form for Words in the Temperley-Lieb Algebra and the Artin Braid
Group on Three Strands

by

Jack Hartsell

The motivation for this thesis is the computer-assisted calculation of the Jones polynomial from braid words in the Artin braid group on three strands, denoted B_3 . The method used for calculation of the Jones polynomial is the original method that was created when the Jones polynomial was first discovered by Vaughan Jones [1] in 1984. This method utilizes the Temperley-Lieb algebra, and in our case the Temperley-Lieb Algebra on three strands, denoted \mathcal{A}_3 , thus generalizations about \mathcal{A}_3 that assist with the process of calculation are pursued.

Copyright by Jack Hartsell 2018
All Rights Reserved

ACKNOWLEDGMENTS

Thanks to Dr. Norwood, for introducing me to mathematics and knot theory and thanks to Dr. Gardner and Dr. Keaton for their assistance and guidance.

TABLE OF CONTENTS

| | |
|--|----|
| ABSTRACT | 2 |
| ACKNOWLEDGMENTS | 4 |
| LIST OF FIGURES | 6 |
| 1 AN INTRODUCTION TO KNOT THEORY AND THE JONES POLY- NOMIAL | 8 |
| 1.1 Knots and Links | 8 |
| 1.2 Computing the Jones Polynomial from the Bracket Polynomial | 12 |
| 2 THE JONES POLYNOMIAL FROM BRAIDS | 16 |
| 2.1 Braids | 16 |
| 2.2 The Artin Braid Group | 18 |
| 2.3 Markov's Theorem | 22 |
| 2.4 The Bracket Polynomial for Braids | 25 |
| 2.5 The Temperley-Lieb Algebra | 27 |
| 2.6 Definitions and Observations | 30 |
| 3 RESULTS | 32 |
| 3.1 Relations in the Temperley-Lieb Algebra | 32 |
| 3.2 Type i and Type ii Curves in the Temperley-Lieb Algebra . . | 34 |
| 3.3 Generalizations of the Artin Braid Group on Three Strands . | 45 |
| 4 FURTHER RESEARCH | 48 |
| BIBLIOGRAPHY | 49 |
| APPENDIX: PYTHON CODE IMPLEMENTATION | 50 |
| VITA | 55 |

LIST OF FIGURES

| | | |
|----|---|----|
| 1 | The Reidemeister Moves | 10 |
| 2 | A Trefoil Knot and its Mirror Image | 11 |
| 3 | Figure Eight Knot | 11 |
| 4 | Crossing Labels, A-split, and B-split | 12 |
| 5 | Trefoil State from Three A-splits | 13 |
| 6 | Bracket Recursion Formula | 13 |
| 7 | Labelling Scheme for Crossings of Oriented Links | 14 |
| 8 | A braid on 3 strands and its closure | 17 |
| 9 | Reidemeister Moves on a 3-braid | 18 |
| 10 | $\sigma_1, \sigma_2,$ and σ_{n-1} | 19 |
| 11 | $\sigma_1^{-1}, \sigma_2^{-1},$ and σ_{n-1}^{-1} | 19 |
| 12 | $\sigma_1, \sigma_2,$ and their concatenation $\sigma_1\sigma_2$ | 19 |
| 13 | The identity element in B_n | 20 |
| 14 | equivalence of $1_3\sigma_1, \sigma_11_3,$ and σ_1 | 20 |
| 15 | $\sigma_i^{-1}\sigma_i = \sigma_i\sigma_i^{-1} = 1_n$ for all $i = 1, 2, \dots, n - 1$ | 20 |
| 16 | Braid Equivalence Example in B_3 | 21 |
| 17 | $\sigma_1\sigma_3 = \sigma_3\sigma_1$ in B_4 | 22 |
| 18 | $\sigma_1^{-1}\sigma_2\sigma_1^{-1}\sigma_2 \in B_3, \sigma_1^{-1}\sigma_2\sigma_1^{-1}\sigma_2\sigma_3 \in B_4,$ and $\sigma_1^{-1}\sigma_2\sigma_1^{-1}\sigma_2\sigma_3^{-1} \in B_4$. . . | 22 |
| 19 | $\overline{\sigma_1^{-1}\sigma_2\sigma_1^{-1}\sigma_2}, \overline{\sigma_1^{-1}\sigma_2\sigma_1^{-1}\sigma_2\sigma_3},$ and $\overline{\sigma_1^{-1}\sigma_2\sigma_1^{-1}\sigma_2\sigma_3^{-1}}$ equivalent by Reidemeister I moves | 23 |
| 20 | $\overline{\sigma_2\sigma_1\sigma_2^{-1}}$ regular isotopic to $\overline{\sigma_1}$ by conjugation | 23 |
| 21 | Bracket Recursion Formula with $B = A^{-1}$ | 25 |

| | | |
|----|---|----|
| 22 | Bracket Recursion Formula for Braids | 26 |
| 23 | Closed Braid State Example | 27 |
| 24 | $U_1U_2U_1 = U_1$ | 28 |
| 25 | $U_1^2 = \delta U_1$ | 29 |
| 26 | $U_1U_3 = U_3U_1$ | 29 |
| 27 | Curve Types of $\overline{U_1^2U_2U_1}$ | 30 |
| 28 | Closures of $1_3, U_1, U_1U_2, U_1U_2U_1,$ and U_2 in \mathcal{A}_3 | 31 |
| 29 | The closure of U_1 in \mathcal{A}_3 | 34 |
| 30 | The closure of U_1^k in \mathcal{A}_3 | 35 |
| 31 | The closure of U_1^{k+1} in \mathcal{A}_3 | 35 |
| 32 | Closures of $\delta^n U_1$ and $\delta^n U_1U_2$ in \mathcal{A}_3 | 37 |
| 33 | U_1 in \mathcal{A}_3 | 38 |
| 34 | U_1^k in \mathcal{A}_3 | 38 |
| 35 | U_1^{k+1} in \mathcal{A}_3 | 39 |
| 36 | U_1U_2 in \mathcal{A}_3 | 40 |
| 37 | $U_1^kU_2$ in \mathcal{A}_3 | 40 |
| 38 | $U_1^{k+1}U_2$ in \mathcal{A}_3 | 41 |
| 39 | $U_1^nU_2^k$ in \mathcal{A}_3 | 42 |
| 40 | $U_1^nU_2^{k+1}$ in \mathcal{A}_3 | 42 |

1 AN INTRODUCTION TO KNOT THEORY AND THE JONES POLYNOMIAL

We are specifically concerned with studying the topological and algebraic properties inherent in knots. The earliest attempts at practical applications of knot theory can be found in the fields of electrodynamics and atomic physics, although neither proved to be fruitful [2]. In spite of this, productive applications of knot theory would eventually be found elsewhere, for which the best known example is Edward Witten's work with the Jones polynomial and its applications to quantum field theory [1].

Towards the purpose of dealing with knots in a more mathematically precise sense, copious definitions and background information are both in order, and will be presented chapters one and two. New results will be proven in chapter three. Possibilities for further research are discussed in chapter four. A Python code implementation using the results for the purpose of calculating the Jones polynomial from a braid word is given as an appendix. Unless otherwise stated, all definitions can be found in [1], [3], and [4].

1.1 Knots and Links

A knot can be intuitively understood by doing the following: with a single piece of string, tie whatever knot may come to mind. Once this knot is created, fuse the two loose ends together, and you now have a knot in a form that we are specifically concerned with. Interlace two or more of these together, and you have a link. With this intuitive understanding in hand, we can now proceed with definitions for the sake of mathematical rigor.

Definition 1.1. [3] A **link** L of m components is a subset of S^3 (the 3-sphere, which is homeomorphic to $R^3 \cup \{\infty\}$) consisting of m disjoint, piecewise linear, simple closed curves. A **knot** K is a link with one component.

Definition 1.2. The **unknot**, also referred to as the trivial knot, is a closed ring with no crossings.

To visually communicate the details of knots or links in a way that is mathematically sound, a precise definition for our pictorial representations is also in order.

Definition 1.3. [1] A **diagram** of a knot or link is a projection of the knot or link onto the plane such that the curves of the knot or link cross transversely, where small segments of the loop are depicted as deleted so as to indicate the locations of crossings.

Definition 1.4. [4] A **homeomorphism** of a space X into another space Y is a bijective continuous function with a continuous inverse. If there exists such a function for two spaces X and Y , we say that these spaces are **homeomorphic**.

The **Jordan Curve Theorem** states that a simple closed curve in the plane separates the plane into two disjoint regions such that each region is homeomorphic to a disc. This theorem makes it possible for our diagrams to represent knots and links with mathematical rigor [1].

Definition 1.5. Two links that are **equivalent** can be continuously deformed from one to the other by some sequence of the three **Reidemeister moves**, which are illustrated in Figure 1. Notice that the first Reidemeister move adds or deletes a single crossing. The second move adds or removes two crossings of the same type

(over or under), and the third move makes no change to the number of crossings. Two diagrams that are equivalent based on all three of the Reidemeister moves are said to be **ambient isotopic**, while two diagrams that are equivalent using only the second and third Reidemeister moves are said to be **regular isotopic**.

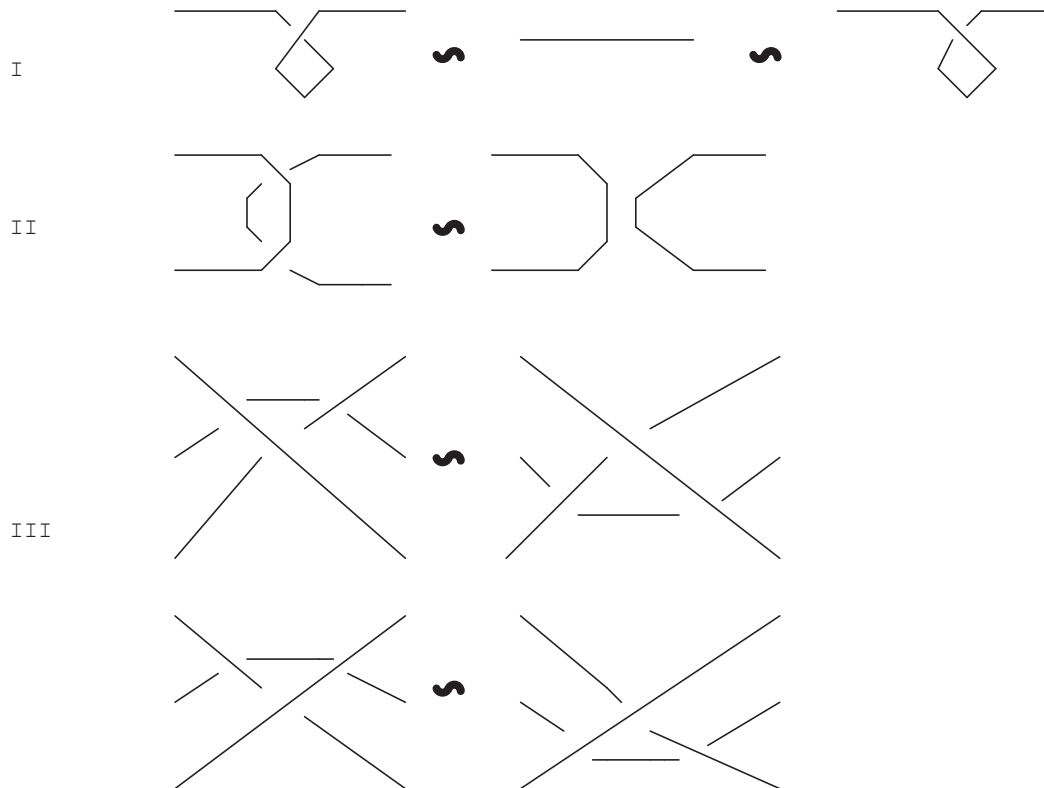


Figure 1: The Reidemeister Moves

Definition 1.6. [1] A **chiral** knot is a knot that is not equivalent to its mirror image. An example of a chiral knot is the trefoil knot, shown in Figure 2 with its mirror image. A knot that isn't chiral is said to be **achiral**, for which the figure eight knot serves as an example shown in Figure 3.

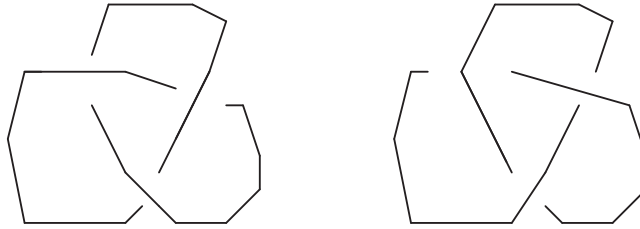


Figure 2: A Trefoil Knot and its Mirror Image

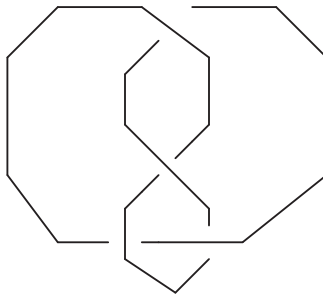


Figure 3: Figure Eight Knot

Since a knot is a simple closed curve, it can be assigned an orientation, which in diagrams will be denoted with arrows along the curve. Clearly there are only two possible ways to orient a knot, and 2^m possible ways of orienting a link of m components [3].

Definition 1.7. [5] An *invariant* of a knot or link is a quantitative expression (almost always a polynomial) that remains unchanged when derived from two equivalent knots or links.

The first such invariant in the history of knot theory was the Alexander polynomial [2]. The motivation for our work is the calculation of the **Jones Polynomial** invented by Vaughn Jones. The Jones Polynomial is noteworthy for being the first

knot invariant capable of distinguishing between the mirror images of chiral knots [1].

1.2 Computing the Jones Polynomial from the Bracket Polynomial

Consider any crossing of a given knot. When following along the under passing strand towards the crossing, label the space left of the strand and in front of the crossing A and the other space B. If one were to cut the knot at this crossing and glue the new pairs of ends back together without recreating the crossing, one would have two choices; you may merge the spaces labelled A together by performing an **A-split**, or you may merge the spaces labelled B together via a **B-split** [1]. This labelling scheme and the two possible operations are illustrated in Figure 4.

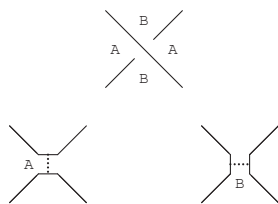


Figure 4: Crossing Labels, A-split, and B-split

This allows for two possible states of the knot after a splitting operation. If this operation is performed on every crossing of a knot with k crossings, we then have 2^k possible states, where each **state** is a collection of Jordan curves in the plane. We will denote a state by σ . Some of these states may be equivalent under isotopy, and some states may be unique [1]. An example of deriving a state of the trefoil knot using three A-splits is shown in Figure 5. The rightmost diagram is the state.

The ability to describe all of these states in a quantitatively meaningful way is sufficient for the calculation of the Jones invariant. For a knot K and a state σ , let

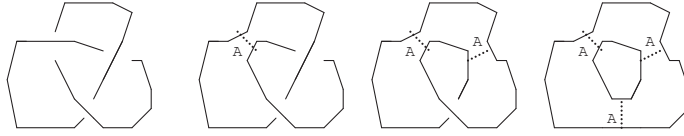


Figure 5: Trefoil State from Three A-splits

$\langle K | \sigma \rangle$ denote the product of the labels of the splitting operations used to derive σ . Using the state σ at the end of Figure 5 as an example, with K the trefoil, we have $\langle K | \sigma \rangle = A^3$. Next, we have that $\|\sigma\| = n - 1$ where n is the number of closed curves in σ . Using the same example, $\|\sigma\| = 2 - 1 = 1$. We can now define the **bracket polynomial** as follows [1]:

$$\langle K \rangle = \sum_{\sigma} \langle K | \sigma \rangle \delta^{|\sigma|}. \quad (1)$$

The bracket polynomial can be computed recursively given the equation illustrated in Figure 6, which should be interpreted as follows: Given three links L , L' , and L'' , where L' and L'' each differ from L at a single crossing by an A -split and a B -split (respectively), the bracket of L is equal to the sum of the bracket of L' multiplied by A and the bracket of L'' multiplied by B [1].

$$\langle L \rangle = \left\langle \begin{array}{c} \diagup \quad \diagdown \\ \diagdown \quad \diagup \end{array} \right\rangle = A \left\langle \begin{array}{c} \diagdown \quad \diagdown \\ \diagup \quad \diagup \end{array} \right\rangle + B \left\langle \begin{array}{c} \diagdown \quad \diagdown \\ \diagdown \quad \diagdown \end{array} \right\rangle = A \langle L' \rangle + B \langle L'' \rangle$$

Figure 6: Bracket Recursion Formula

When we set $B = A^{-1}$ and $\delta = -A^2 - A^{-2}$, the bracket is an invariant under type II and III Reidemeister moves, and thus an invariant of regular isotopy. If we want

invariance of ambient isotopy, we will need to normalize the bracket polynomial.

Definition 1.8. [1] For an oriented link K , the **writhe** of K , $w(K)$, is the sum of the labels of the link's crossings given the following labelling scheme: given a vertical alignment of the crossing using the orientation, we label the crossing $+1$ if the overcrossing has a positive slope, and -1 if the overcrossing slope is negative, as shown in Figure 7.

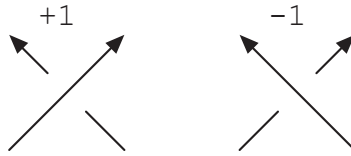


Figure 7: Labelling Scheme for Crossings of Oriented Links

We can now define the **normalized bracket** \mathcal{L}_K of a link K , which is an invariant of ambient isotopy [1]:

$$\mathcal{L}_K = (-A^3)^{-w(K)} \langle K \rangle. \quad (2)$$

Definition 1.9. [1] The **Jones polynomial** $V_K(t)$ of an oriented link K is a polynomial of finite length in the single variable \sqrt{t} with integer coefficients, where \sqrt{t} can have either positive or negative exponents, satisfying the following properties:

- 1) K ambient isotopic to K' implies $V_K(t) = V_{K'}(t)$.
- 2) If K is the unknot, then $V_K(t) = 1$.
- 3) If K and K' differ only at a single crossing, such that the crossing would be labelled positive in K and negative in K' using the scheme described earlier,

then $t^{-1}V_K - tV_{K'} = (\sqrt{t} - \frac{1}{\sqrt{t}})K''$, where K'' is a knot obtained from K via an A -split at the aforementioned crossing.

[3] The Jones polynomial can be derived from the normalized bracket via the substitution of an indeterminate t described in the following equation:

$$V_K(t) = \left((-A)^{-3w(K)} \langle K \rangle \right)_{t^{1/2}=A^{-2}} \in \mathbb{Z}[t^{-1/2}, t^{1/2}]. \quad (3)$$

2 THE JONES POLYNOMIAL FROM BRAIDS

2.1 Braids

The concept of a **braid** is necessary for the method of calculating the Jones Polynomial that will be utilized later in this thesis. Braids can readily be considered in the most intuitive means available to anyone who has braided hair, which is especially convenient since the work herein is specifically considered with braids on three strands.

Definition 2.1. *A **braid** b on n strands is a set of n pairwise disjoint curves such that each strand has exactly one endpoint in each of two parallel planes A and B , and any plane parallel to A and B will intersect each strand either once or not at all.*

As with pictorial representations of knots, a mathematically meaningful definition for visualizations of braids follows similarly.

Definition 2.2. *A **diagram** of a braid b is a projection of a braid onto two-dimensional space, such that the same properties as in the definition of a diagram of a knot or link are satisfied.*

With this pictorial representation of braids, we can begin to consider a more simplified means of contemplating them. The parallel planes mentioned earlier in the definition of a braid can be simplified to parallel lines, with n points evenly spaced across each of them directly above or below their corresponding point at the opposite line. With this in mind, it may be simpler to intuitively visualize the closure of a braid.

Definition 2.3. [1]A **closed braid** \bar{b} is formed from a braid b by connecting the

n points of origin at plane *A* to their corresponding endpoints at plane *B* without creating any crossings.

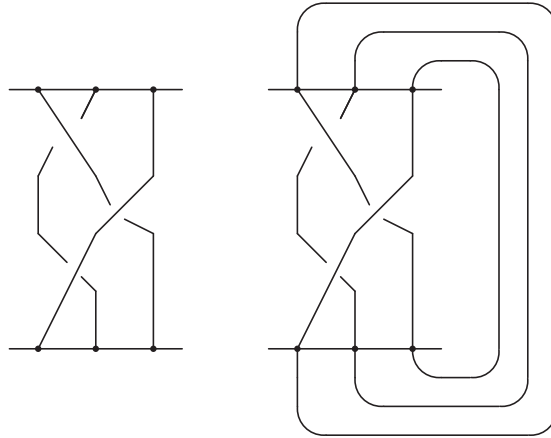


Figure 8: A braid on 3 strands and its closure

Braids are useful for two reasons: their closure is a link, and they have a useful algebraic structure, which will be discussed later. As for knot equivalence, we can make use of **Alexander's Theorem**, which states that each link in three-dimensional space is ambient isotopic to a link in the form of a closed braid. That is, each link is equivalent under the Reidemeister moves to a closed braid [1]. If two braids b and b' are both equivalent to the same link by Alexander's Theorem, then clearly the closures \bar{b} and \bar{b}' will be ambient isotopic to one another. Note that two braids need not be equivalent to one another for their closures to both be ambient isotopic to the same link, and thus ambient isotopic to each other. There is much to gain from being able to rigorously describe the relationship between two such braids. That is, given $b_n \in B_n$ and $b'_m \in B_m$ such that \bar{b}_n and \bar{b}'_m are ambient isotopic, where m and n may or may not be equal, it will be useful to have a method for obtaining b_n from b'_m .

2.2 The Artin Braid Group

Consider the set of all equivalence classes of braids, where two braids are equivalent if they can be continuously deformed into one another via the Reidemeister moves without moving the start or end points of the strands, and without moving the strands outside of the space between the two parallel planes containing the end points, as illustrated in Figure 9. Note that the Type I Reidemeister move is not useful to us for this definition of braid equivalence, since the definition of a braid forbids strands from doubling back toward their plane of origin.

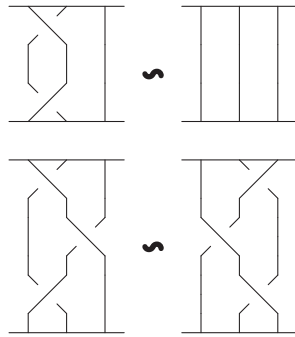


Figure 9: Reidemeister Moves on a 3-braid

This set of equivalence classes of braids is the set on which the Artin braid group B_n is defined. The group is generated by elements σ_i , which are braids where the i -th strand crosses under the $i + 1$ -st strand, and the inverse of this generator is σ_i^{-1} , the braid where the i -th strand crosses over the $i + 1$ -st strand. We refer to a sequence of such generators as a **braid word**.

The binary operation of the group is concatenation of braids, a stacked arrangement of braids so that the end points of the first braid coincide with the starting

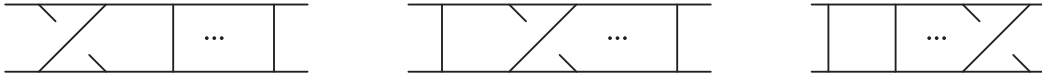


Figure 10: σ_1 , σ_2 , and σ_{n-1}

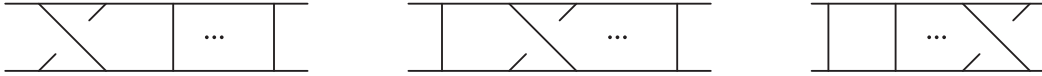


Figure 11: σ_1^{-1} , σ_2^{-1} , and σ_{n-1}^{-1}

points of the second braid, and so on. This is illustrated in Figure 12.

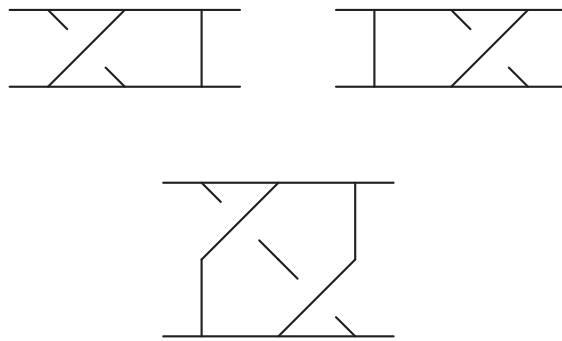


Figure 12: σ_1 , σ_2 , and their concatenation $\sigma_1\sigma_2$

Towards showing that B_n satisfied the axioms of a group, we observe that a two-sided identity element exists in the form of an unbraid. The unbraid is a braid analogue to the unknot, their common property being the lack of crossings. This identity element is illustrated in Figures 13 and 14.

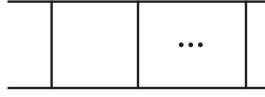


Figure 13: The identity element in B_n

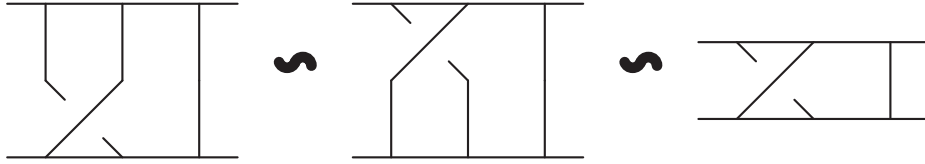


Figure 14: equivalence of $1_3\sigma_1$, σ_11_3 , and σ_1

We also have that each σ_i has a two-sided inverse σ_i^{-1} . The equivalence of $\sigma_i\sigma_i^{-1}$ and $\sigma_i^{-1}\sigma_i$ with the identity in B_n is illustrated in Figure 15.

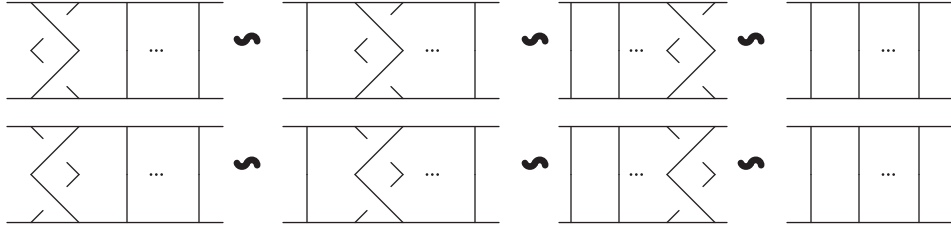


Figure 15: $\sigma_i^{-1}\sigma_i = \sigma_i\sigma_i^{-1} = 1_n$ for all $i = 1, 2, \dots, n - 1$

Concatenation is also associative, so the axioms of a group are satisfied by the Artin braid group. This braid group is defined with the aforementioned generators and the following relations:

$$\begin{aligned} \sigma_i \sigma_i^{-1} &= \sigma_i^{-1} \sigma_i = 1 \quad i = 1, 2, \dots, n - 1, \\ \sigma_i \sigma_{i+1} \sigma_i &= \sigma_{i+1} \sigma_i \sigma_{i+1} \quad i = 1, 2, \dots, n - 1, \\ \sigma_i \sigma_j &= \sigma_j \sigma_i \quad |i - j| > 1. \end{aligned} \tag{4}$$

The first and second relations describe equivalence under type II and type III Reidemeister moves, respectively. An example of using these relations to establish equivalence with the identity in B_3 is shown in Figure 16.

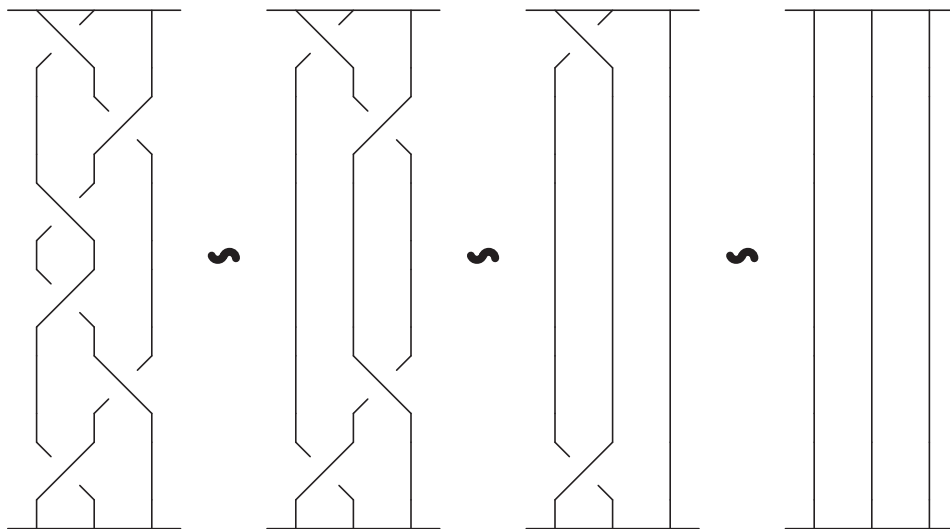


Figure 16: Braid Equivalence Example in B_3

The third relation gives us that two consecutive crossings on disjoint pairs of strands in a braid can commute with one another by merely sliding the crossings vertically, as illustrated in Figure 17.



Figure 17: $\sigma_1\sigma_3 = \sigma_3\sigma_1$ in B_4

2.3 Markov's Theorem

We can now describe two other means of manipulating braids to produce other braids with ambient isotopic closures. One is a **Markov Move**: for a given braid b in B_n , if a strand is added to b which has one crossing of the last strand in b , so that it is then a braid in B_{n+1} , then $\overline{b\sigma_n}$, $\overline{b\sigma_n^{-1}}$, and \overline{b} are ambient isotopic to one another [1]. An example using $\sigma_1^{-1}\sigma_2\sigma_1^{-1}\sigma_2 \in B_3$ and $\sigma_3, \sigma_3^{-1} \in B_4$ is shown in Figure 18, where their closures can be seen as equivalent in Figure 19 by type I Reidemeister moves.

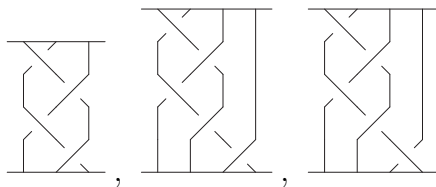


Figure 18: $\sigma_1^{-1}\sigma_2\sigma_1^{-1}\sigma_2 \in B_3$, $\sigma_1^{-1}\sigma_2\sigma_1^{-1}\sigma_2\sigma_3 \in B_4$, and $\sigma_1^{-1}\sigma_2\sigma_1^{-1}\sigma_2\sigma_3^{-1} \in B_4$

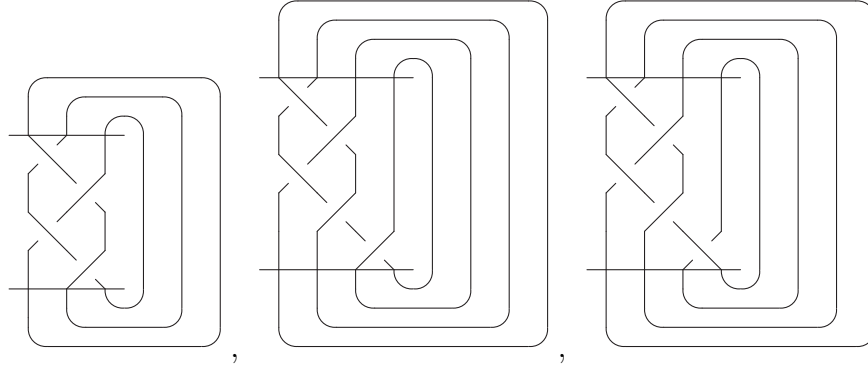


Figure 19: $\overline{\sigma_1^{-1}\sigma_2\sigma_1^{-1}\sigma_2}$, $\overline{\sigma_1^{-1}\sigma_2\sigma_1^{-1}\sigma_2\sigma_3}$, and $\overline{\sigma_1^{-1}\sigma_2\sigma_1^{-1}\sigma_2\sigma_3^{-1}}$ equivalent by Reidemeister I moves

A second move for obtaining braids with ambient isotopic closures is **braid conjugation**. Given two braids b and b' in B_n , if we concatenate b , b' , and b^{-1} to get $bb'b^{-1}$, b will cancel with its inverse in the closure of $bb'b^{-1}$ (though not in the braid group), thus making $\overline{bb'b^{-1}}$ ambient isotopic to $\overline{b'}$ [1]. An example using two braids in B_3 is shown in Figure 20.

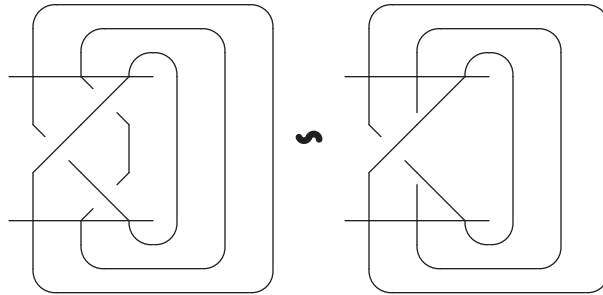


Figure 20: $\overline{\sigma_2\sigma_1\sigma_2^{-1}}$ regular isotopic to $\overline{\sigma_1}$ by conjugation

These two moves for manipulating braids are critical to the statement of the following theorem:

Theorem 2.4. Markov Theorem [1] *Let $b_n \in B_n$ and $b'_m \in B_m$ be two braids in the braid groups B_n and B_m , and let $\overline{b_n}$ and $\overline{b'_m}$ be their respective closures. Then, two links $L = \overline{b_n}$ and $L' = \overline{b'_m}$ are ambient isotopic if and only if b'_m can be obtained from b_n by a series of:*

- 1) *equivalences in a given braid group.*
- 2) *conjugation in a given braid group.*
- 3) *Markov moves or inverse Markov moves.*

The Markov Theorem allows us to use presentations of braid groups to calculate link invariants. A **Markov trace** on $\{B_n\}$ is a family of functions $\{J_n\}$ where $J_n : B_n \rightarrow R$, $n \in \mathbb{N} \setminus \{1\}$, and R is a commutative ring, such that all $J_n \in \{J_n\}$ satisfy the following conditions [1]:

- 1) J_n is well defined for all $b \in B_n$.
- 2) If $a, b \in B_n$, then $J_n(b) = J_n(aba^{-1})$ (satisfying equivalence under braid conjugation).
- 3) For all $b \in B_n$, there exists $\alpha \in R$ that does not depend on n for which $J_{n+1}(b\sigma_n) = \alpha J_n(b)$ and $J_{n+1}(b\sigma_n^{-1}) = \alpha^{-1} J_n(b)$ both hold (satisfying equivalence under a Markov move).

Before we can use the Markov trace to construct invariants, we need to define the **writhe** of a braid, $w(b)$, which is equal to the exponent sum of the braid's factors.

More explicitly, for a braid word $b = \sigma_{i_1}^{a_1} \sigma_{i_2}^{a_2} \dots \sigma_{i_k}^{a_k}$:

$$w(b) = \sum_{l=1}^k a_l. \tag{5}$$

For a braid b in B_n , a link L ambient isotopic to a closed braid \bar{b} by Alexander's Theorem, and R a commutative ring, we define the **link invariant for the Markov trace** by:

$$J(L) = \alpha^{-w(b)} J_n(b) \in R. \tag{6}$$

The link invariant for the Markov trace is in fact an invariant of ambient isotopy for oriented links, such that if L and L' are links equivalent under ambient isotopy, then $J(L) = J(L')$ [1].

2.4 The Bracket Polynomial for Braids

The bracket for closed braids can be considered in terms of the link invariant of the Markov trace. Let $R = \mathbb{Z}[A, A^{-1}]$, so that we have $J_n : B_n \rightarrow \mathbb{Z}[A, A^{-1}]$ such that $J_n(b) = \langle \bar{b} \rangle$. Consider the bracket recursion formula with $B = A^{-1}$, as shown in Figure 21.

$$\langle \text{crossing} \rangle = A \langle \text{no crossing} \rangle + A^{-1} \langle \text{crossing} \rangle$$

Figure 21: Bracket Recursion Formula with $B = A^{-1}$

$$\langle \text{||} \dots | \text{ } \diagdown \text{ } \diagup \text{ } | \dots \text{||} \rangle = A \langle \text{||} \dots \text{||} \text{||} \text{||} \dots \text{||} \rangle + A^{-1} \langle \text{||} \dots | \text{ } \cup \text{ } | \dots \text{||} \rangle$$

Figure 22: Bracket Recursion Formula for Braids

This recursion formula can then be applied to braids by considering each ‘step’ in the braid word in the same way that we consider each crossing in a link, such that the recursion formula should be considered as illustrated in Figure 22. If we let U_i denote the ‘cup-cap’ formation caused by a B -split in a braid’s crossing at strands i and $i + 1$, we can define the bracket recursion formula as follows:

$$\langle \sigma_i \rangle = A \langle 1_n \rangle + A^{-1} \langle U_i \rangle. \quad (7)$$

Since states are defined in a way that requires all crossings to be resolved by splits, a state of a closed braid will thus be defined solely in terms of these new elements U_i . An example of one possible state of $\overline{\sigma_1^2 \sigma_2 \sigma_1}$ is shown in Figure 23 as $\overline{U_1^2 U_2 U_1}$.

In much the same way as was done with the number of closed curves in a state of a link, we define $\|s\| = n - 1$, where s is a braid state given by an arbitrary product of U_i ’s and n is the number of closed curves in the closure of the product. We can then go on to define the bracket for braids. Let $\delta = -A^2 - A^{-2}$. For a braid b and a state s , let $\langle b | s \rangle$ denote the product of the A ’s and A^{-1} ’s associated with the state s . Using the state shown in Figure 23 as an example state for $b = \sigma_1^2 \sigma_2 \sigma_1$, we have $\langle b | s \rangle = A^{-4}$. Using this same example, we will have that $|s| = 3 - 1 = 2$. Then with

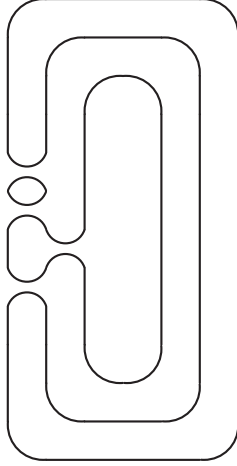


Figure 23: Closed Braid State Example

s used as the index for our states, the bracket for a braid b is defined as:

$$\langle b \rangle = \sum_s \langle b | s \rangle \delta^{\|s\|}. \quad (8)$$

The normalized bracket for a braid \mathcal{L}_b is similarly defined as that for a knot or link. Using the writhe of the braid $w(b)$ we define \mathcal{L}_b as follows:

$$\mathcal{L}_b = (-A^3)^{-w(b)} \langle b \rangle. \quad (9)$$

We can now proceed to further define an algebraic structure which will be used as a representation of a braid group.

2.5 The Temperley-Lieb Algebra

Definition 2.5. [1] A **Laurent polynomial** is a polynomial with finitely many positive and negative powers of an indeterminate x with coefficients in a field \mathbb{F} .

Definition 2.6. [1] The **Temperley-Lieb Algebra** \mathcal{A}_n is a module over the ring of Laurent polynomials $\mathbb{Z}[A, A^{-1}]$ with a designated loop value defined by $\delta = -A^2 - A^{-2} \in \mathbb{Z}[A, A^{-1}]$. It is generated by elements U_1, U_2, \dots, U_{n-1} , and a sequence of these elements is referred to as a word in \mathcal{A}_n . Diagrammatically, U_i plays a similar role to that of σ_i in the Artin braid group, with the notable difference being a ‘cup-cap’ formation at strands i and $i + 1$ instead of a crossing of the two strands.

Definition 2.7. [1] A **Temperley-Lieb diagram** is a projection onto two-dimensional space of the set of pairwise disjoint curves formed by the generators of the Temperley-Lieb algebra, such that $2n$ pairs of points split evenly along two parallel lines will be connected in pairs. All curves are drawn in the space between the two parallel lines, and no two curves intersect or cross one another. The **closure** of a Temperley-Lieb diagram is essentially the same as that for braid diagrams.

We have the following relations in \mathcal{A}_n [1], diagrams for which are illustrated in Figures 24, 25, and 26 respectively:

$$U_i U_{i\pm 1} U_i = U_i,$$

$$U_i^2 = \delta U_i, \text{ where } \delta = -A^2 - A^{-2}, \tag{10}$$

$$U_i U_j = U_j U_i \text{ if } |i - j| > 1.$$

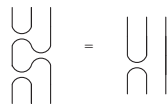


Figure 24: $U_1 U_2 U_1 = U_1$

$$\begin{array}{c} \cup \\ \circ \\ \cap \end{array} \Big| = \circ \begin{array}{c} \cup \\ \cap \end{array} \Big|$$

Figure 25: $U_1^2 = \delta U_1$

$$\begin{array}{c} \cup \\ \cap \end{array} \begin{array}{c} \cup \\ \cap \end{array} = \begin{array}{c} \cup \\ \cup \\ \cap \\ \cap \end{array}$$

Figure 26: $U_1 U_3 = U_3 U_1$

Given these relations in a module, it is important to note that we do not have commutativity of elements U_i, U_j when $|i - j| = 1$. This effectively means that we do not have commutativity of any sort when we restrict our observations to \mathcal{A}_3 .

With the Temperley-Lieb algebra, we can now define a mapping $\rho : B_n \rightarrow \mathcal{A}_n$ by the following:

$$\begin{aligned} \rho(\sigma_i) &= A + A^{-1}U_i, \\ \rho(\sigma_i^{-1}) &= AU_i + A^{-1}. \end{aligned} \tag{11}$$

It follows that for a braid b , and U_s the product of U_i 's for a given state s of a braid:

$$\rho(b) = \sum_s \langle b \mid s \rangle U_s. \tag{12}$$

We use this mapping in terms of the link invariant of the Markov trace in much the same way we did earlier, by defining $J_n : \mathcal{A}_n \rightarrow \mathbb{Z}[A, A^{-1}]$ by $J_n(\rho(b)) = \langle b \rangle$. More specifically,

$$J_n(\rho(b)) = \sum_s \langle b \mid s \rangle \langle U_s \rangle = \sum_s \langle b \mid s \rangle \delta^{\|s\|}. \tag{13}$$

The Jones polynomial can then be derived from this version of the normalized bracket as was already shown.

2.6 Definitions and Observations

Much of the work herein is only valid when restricted to braids on three strands. Given the closure of a diagram generated by elements U_i in \mathcal{A}_3 , which we will denote $\overline{U_i}$, there exist two types of closed curves, which are labelled in Figure 27 as follows:

- i. closed curves formed by the ‘cup-cap’ relationship of repeated elements U_i with the same i ,
- ii. closed curves formed by the closure of the sequence of U_i 's.

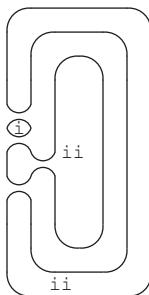


Figure 27: Curve Types of $\overline{U_1^2 U_2 U_1}$

The number of curves of the second type is dependent upon:

- a. the number of strands n in the braid from which we have derived the resultant element of the Temperley-Lieb Algebra \mathcal{A}_n .
- b. the ‘‘collapsed length’’ of the word in \mathcal{A}_3 . That is, the length γ of a word

$$\overline{U_{k_1}^{j_1} U_{k_2}^{j_2} \dots U_{k_\gamma}^{j_\gamma}} \text{ such that } k_i \neq k_{i+1} \text{ for all } i = 1, \dots, \gamma - 1.$$

Clearly, the number of closed curves of type ii can not exceed the number n from \mathcal{A}_n .

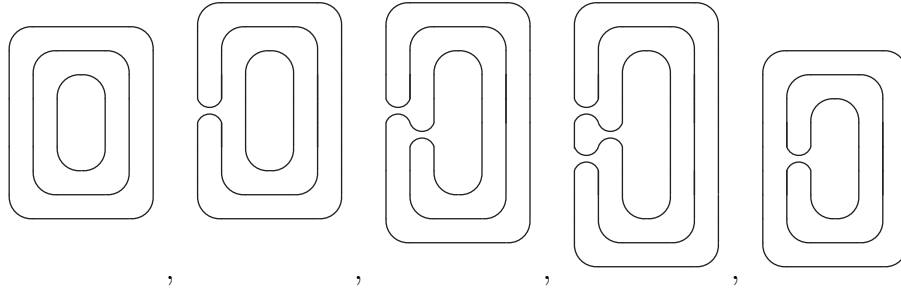


Figure 28: Closures of 1_3 , U_1 , U_1U_2 , $U_1U_2U_1$, and U_2 in \mathcal{A}_3

We will eventually prove that for a diagram of the closure of a word in \mathcal{A}_3 of the form $\overline{U_{k_1}^{j_1}U_{k_2}^{j_2}\dots U_{k_\gamma}^{j_\gamma}}$, $k_i \neq k_{i+1}$ for all $i = 1, \dots, \gamma - 1$, the total number of curves is a function of both the “collapsed length” γ and the sum of the exponents $\alpha = \sum_{i=1}^n j_i$.

Furthermore, when dealing with the Artin-Braid group, we will denote equivalence of the closures of two braid words by \equiv_c , and the set of all braid closures on three strands as $\overline{B_3}$.

3 RESULTS

3.1 Relations in the Temperley-Lieb Algebra

Our first theorem is noteworthy in that it provides a generalization that holds for \mathcal{A}_n , thus holding for any arbitrary number of strands n in the Temperley-Lieb Algebra, whereas the rest of the work in this thesis is only proven to hold for 3 strands.

Theorem 3.1. *In \mathcal{A}_n , given a word of the form $U_{k_1}^{j_1}U_{k_2}^{j_2}\dots U_{k_\gamma}^{j_\gamma}$, and the exponent sum defined by $\alpha = \sum_{i=1}^{\gamma} j_i$, $U_{k_1}^{j_1}U_{k_2}^{j_2}\dots U_{k_\gamma}^{j_\gamma} = \delta^{\alpha-\gamma}U_{k_1}U_{k_2}\dots U_{k_\gamma}$.*

Proof. Recall the following relation

$$U_i^2 = \delta U_i. \tag{14}$$

The proof then follows from the computation given below.

$$\begin{aligned} U_{k_1}^{j_1}U_{k_2}^{j_2}\dots U_{k_\gamma}^{j_\gamma} &= \delta^{j_1-1}U_{k_1}\delta^{j_2-1}U_{k_2}\dots\delta^{j_\gamma-1}U_{k_\gamma} \\ &= (\delta^{j_1-1}\delta^{j_2-1}\dots\delta^{j_\gamma-1})U_{k_1}U_{k_2}\dots U_{k_\gamma} \\ &= \delta^{(j_1-1)+(j_2-1)+\dots+(j_\gamma-1)}U_{k_1}U_{k_2}\dots U_{k_\gamma} \\ &= \delta^{\alpha-\gamma}U_{k_1}U_{k_2}\dots U_{k_\gamma}. \end{aligned} \tag{15}$$

□

The next theorem allows us to restrict our attention to words of the form U_i or U_iU_j , $i \neq j$, whenever we are given a word of the form $U_{k_1}U_{k_2}\dots U_{k_\gamma}$, $k \neq k+1$ for all $k = 1, 2, \dots, \gamma-1$. In fact, we will frequently be combining the next theorem with the

previous one to generalize words of “reduced” form $U_{k_1}^{j_1} U_{k_2}^{j_2} \dots U_{k_\gamma}^{j_\gamma}$ given an equivalence to either $\delta^m U_i U_j$ or $\delta^m U_i$, for $i \neq j$ and m in the natural numbers union zero.

Theorem 3.2. *For a word of the form $U_{k_1} U_{k_2} \dots U_{k_\gamma}$, $k_i \neq k_{i+1}$ for all $i = 1, \dots, \gamma - 1$, $\gamma > 0$, in \mathcal{A}_3 , if γ is even, then $U_{k_1} U_{k_2} \dots U_{k_\gamma} = U_{k_1} U_{k_2}$, and if γ is odd, $U_{k_1} U_{k_2} \dots U_{k_\gamma} = U_{k_1}$.*

Proof. Without loss of generality let $U_{k_1} = U_1$ in all cases. Consider the case where γ is even. Then $U_{k_\gamma} = U_2$. Proceeding by induction, in the case where $\gamma = 2$, our theorem immediately holds. Suppose the theorem holds for some even $\gamma = n > 2$, such that $U_{k_1} U_{k_2} \dots U_{k_n} = U_1 U_2 \dots U_2 = U_1 U_2$.

$$\begin{aligned}
U_{k_1} U_{k_2} \dots U_{k_{n+2}} &= U_1 U_2 \dots U_2 U_1 U_2 \\
&= (U_1 U_2 \dots U_2) U_1 U_2 \\
&= U_1 U_2 U_1 U_2 \\
&= U_1 (U_2 U_1 U_2) \\
&= U_1 U_2.
\end{aligned} \tag{16}$$

Next, consider the case where γ is odd. Then $U_{k_\gamma} = U_1$. Proceeding by induction, in the case where $\gamma = 1$, our theorem immediately holds. Suppose our theorem holds for some odd $\gamma = n > 1$, such that $U_{k_1} U_{k_2} \dots U_{k_n} = U_1 U_2 \dots U_1 = U_1$.

$$\begin{aligned}
U_{k_1} U_{k_2} \dots U_{k_{n+2}} &= U_1 U_2 \dots U_1 U_2 U_1 \\
&= (U_1 U_2 \dots U_1) U_2 U_1 \\
&= U_1 U_2 U_1 = U_1.
\end{aligned} \tag{17}$$

□

3.2 Type i and Type ii Curves in the Temperley-Lieb Algebra

The bracket polynomial is dependent on the number of closed curves in a diagram of a resolved state of a knot or link. We observed in chapter two that all curves in \mathcal{A}_3 can be classified as one of two types. In Theorems 3.3, 3.4, 3.5, and 3.6 we will arrive at generalizations regarding the total number of curves of the first type, which are curves described as being formed by the ‘cup-cap’ relationship of sequential terms U_i . Theorem 3.3 establishes the relationship between consecutive terms U_i and the formation of type i curves by considering only words of a single factor raised to the power of an arbitrary natural number n .

Theorem 3.3. *The number of type i curves in the closure of diagrams of the form U_i^n , $n > 0$ in \mathcal{A}_3 is equal to $n - 1$.*

Proof. Without loss of generality, consider U_1^n . Suppose $n = 1$. Then for U_1 , we have zero curves of type i as shown in Figure 29.



Figure 29: The closure of U_1 in \mathcal{A}_3

Suppose our theorem holds for $n = k$ so that the diagram shown in Figure 30 has $k - 1$ curves of type i.

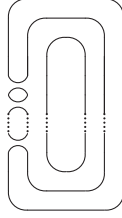


Figure 30: The closure of U_1^k in \mathcal{A}_3

Then, for $k + 1$, note that $U_1^{k+1} = U_1^k U_1$.

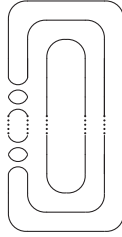


Figure 31: The closure of U_1^{k+1} in \mathcal{A}_3

We can observe Figure 31 shows that there is one additional type i curve. Thus the number of type i curves for $n = k + 1$ is therefore $(k - 1) + 1 = k = n - 1$. \square

Now that we have established that the relationship between the formation of type i curves and the sequential multiplication of the same generator U_i in \mathcal{A}_3 , we can take advantage of the relation $U_i^2 = \delta U_i$ to give us a result that yields the number of type i curves given the exponent of δ .

Corollary 3.4. *The number of type i curves in the closure of diagrams of $\delta^m U_i$ in \mathcal{A}_3 is equal to m .*

Proof. Recall the following relation

$$U_i^2 = \delta U_i. \tag{18}$$

It then immediately follows from this relation that $\delta^m U_i = U_i^{m+1}$. Then, for $m = n-1$, the proof follows from Theorem 3.3. \square

The next theorem begins by confirming that when we right multiply $\delta^m U_i$ by U_j in \mathcal{A}_3 , for $i \neq j$, the number of type i curves is not affected. It is then shown by induction that right multiplying in this alternating fashion can be performed an arbitrary number of times without having any effect on the number of type i curves. Thus it is shown that the number of type i curves in a diagram of the closure of a word of this form is only dependent on the value of the exponent on δ .

Theorem 3.5. *In \mathcal{A}_3 , given a diagram of the form $\delta^n U_{k_1} U_{k_2} \dots U_{k_\gamma}$, $k_i \neq k_{i+1}$ for all $i = 1, \dots, \gamma - 1$, the number of type i curves will be equal to n .*

Proof. Recall from Corollary 3.4 that, given $\delta^n U_i$, there will exist n curves of type i . In the case where γ is odd, given Theorem 3.2 we have that $\delta^n U_{k_1} U_{k_2} \dots U_{k_\gamma} = \delta^n U_{k_1}$. Thus our theorem immediately holds for the case where γ is odd.

In the case where γ is even, recall from Theorem 3.2 that $\delta^n U_{k_1} U_{k_2} \dots U_{k_\gamma} = \delta^n U_{k_1} U_{k_2}$.

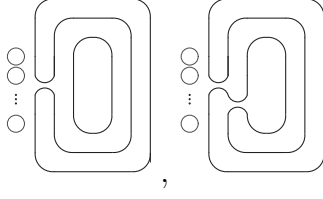


Figure 32: Closures of $\delta^n U_1$ and $\delta^n U_1 U_2$ in \mathcal{A}_3

Without loss of generality, let $U_{k_1} = U_1$ and $U_{k_2} = U_2$. The diagram in Figure 32 shows that, when $\delta^n U_1$ is right multiplied by U_2 , no new type i curves are created or destroyed, and thus our theorem holds. □

The last result regarding type i curves in this chapter generalizes our calculation of type i curves for all words of a reduced form in \mathcal{A}_3 by equivalence with a word satisfying the conditions of Theorem 3.5.

Theorem 3.6. *In \mathcal{A}_3 , given a diagram of the form $U_{k_1}^{j_1} U_{k_2}^{j_2} \dots U_{k_\gamma}^{j_\gamma}$, $k_i \neq k_{i+1}$ for all $i = 1, \dots, \gamma - 1$, and $\alpha = \sum_{i=1}^n j_i$, the number of type i curves will be equal to $\alpha - \gamma$.*

Proof. From Theorem 3.1, we have that $U_{k_1}^{j_1} U_{k_2}^{j_2} \dots U_{k_\gamma}^{j_\gamma} = \delta^{\alpha-\gamma} U_{k_1} U_{k_2} \dots U_{k_\gamma}$. Therefore our proof follows from Theorem 3.5 for $n = \alpha - \gamma$. □

The remaining results of this section establish that the number of type ii curves in diagrams from words in \mathcal{A}_3 is dependent only on the length of the word in 'reduced' form, that is, a word of a form $U_{k_1}^{j_1} U_{k_2}^{j_2} \dots U_{k_\gamma}^{j_\gamma}$ such that $k_i \neq k_{i+1}$ for all $i = 1, 2, \dots, \gamma - 1$. We begin to isolate this dependence on the 'reduced length', γ , by showing that the number of type ii curves is independent of the exponential values of the generators in

a word. The first such proof begins by showing this independence to hold for a word where γ is equal to one.

Theorem 3.7. *The number of type ii curves in the closure of diagrams of U_i^n in \mathcal{A}_3 is equal to 2.*

Proof. Without loss of generality, consider U_1^n . Suppose $n = 1$. Then for U_1 , we have two curves of type ii, as shown in Figure 33.

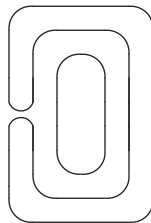


Figure 33: U_1 in \mathcal{A}_3

Suppose our theorem holds for $n = k$ so that the diagram in Figure 34 has two curves of type ii.

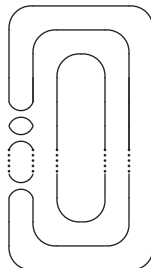


Figure 34: U_1^k in \mathcal{A}_3

Then, for $k + 1$, note that $U_1^{k+1} = U_1^k U_1$.

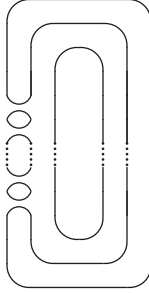


Figure 35: U_1^{k+1} in \mathcal{A}_3

Since no such additional curves are formed in the closure of the diagram shown in Figure 35, we can conclude that there are two curves of type ii, and therefore the theorem holds. \square

Corollary 3.8. *The number of type ii curves in the closure of diagrams of $\delta^m U_i$ in \mathcal{A}_3 is equal to 2.*

Proof. Recall the relation $U_i^2 = \delta U_i$. This gives us that $\delta^m U_i = U_i^{m+1}$, where for $n = m + 1$ Theorem 3.7 allows us to conclude that there are therefore 2 type ii curves. \square

Now that the number of type ii curves has been shown to be independent of exponents in words where γ is equal to one, Theorems 3.9, 3.10, 3.11, and 3.12 continue to confirm this independence to hold for all cases of words where γ is equal to two.

Theorem 3.9. *The number of type ii curves in the closure of diagrams of $U_i^n U_j$, $i \neq j$, $n > 0$, in \mathcal{A}_3 is equal to 1.*

Proof. Without loss of generality, consider $U_1^n U_2$. Suppose $n = 1$. Then for $U_1 U_2$, we can observe there is one curve of type ii, as shown in Figure 36.

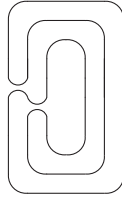


Figure 36: $U_1 U_2$ in \mathcal{A}_3

Suppose our theorem holds for $n = k$ so that the diagram in Figure 37 has one curve of type ii.

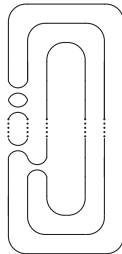


Figure 37: $U_1^k U_2$ in \mathcal{A}_3

Then, for $k + 1$, note that $U_1^{k+1} U_2 = U_1^k U_1 U_2$.

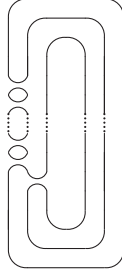


Figure 38: $U_1^{k+1}U_2$ in \mathcal{A}_3

Since no such additional curves are formed in the closure of the diagram as shown in Figure 38, we can conclude that there is one curve of type ii, and therefore the theorem holds. \square

Theorem 3.10. *The number of type ii curves in the closure of diagrams of $U_iU_j^n$, $i \neq j$, $n > 0$, in \mathcal{A}_3 is equal to 1.*

Proof. The proof is essentially identical to the proof of Theorem 3.9. \square

Corollary 3.11. *The number of type ii curves in the closure of diagrams of $\delta^m U_i U_j$, $i \neq j$, $m > 0$, in \mathcal{A}_3 is equal to 1.*

Proof. Given the relation that yields $\delta^m U_i U_j = U_i^{m+1} U_j$, the proof follows immediately from Theorem 3.9. \square

Theorem 3.12. *The number of type ii curves in the closure of diagrams of $U_i^n U_j^m$, $i \neq j$, $n > 0$, in \mathcal{A}_3 is equal to 1.*

Proof. Without loss of generality, consider $U_1^n U_2^m$. Suppose $m = 1$. In Theorem 3.9 we showed that the diagram of $U_1^n U_2$ has only one type ii curve, and thus the theorem

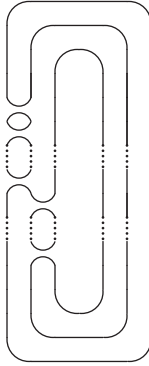


Figure 39: $U_1^n U_2^k$ in \mathcal{A}_3

holds for the base case. Suppose our theorem holds for $m = k$ so that the diagram in Figure 39 has one curve of type ii.

Then, for $k + 1$, note that $U_1^n U_2^{k+1} = U_1^n U_2^k U_2$.

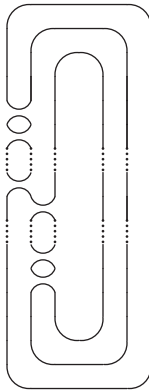


Figure 40: $U_1^n U_2^{k+1}$ in \mathcal{A}_3

Since no additional type ii curves are formed in the closure of the diagram as shown in Figure 40, we can conclude that there is one curve of type ii, and therefore the theorem holds. □

Now that it is established that the number of type ii curves is independent of exponents in words such that γ is equal to one or two, the next theorem will show us that the number of type ii curves is dependent on the parity of γ . The case of a word with generators raised to a power greater than one is ignored for now for the sake of observing this dependence on parity in isolation.

Theorem 3.13. *For a word of the form $U_{k_1}U_{k_2}\dots U_{k_\gamma}$, $k_i \neq k_{i+1}$ for all $i = 1, \dots, \gamma - 1$, in \mathcal{A}_3 , if γ is even, then the number of type ii curves in the diagram is equal to 1, and if γ is odd, then the number of type ii curves in the diagram is equal to 2.*

Proof. Without loss of generality let $U_{k_1} = U_1$. Consider the case where γ is even. Then $U_{k_\gamma} = U_2$. Consider the case where $\gamma = 2$. We have already shown the theorem to hold in this case. Let us further consider $\gamma = 4$. Then our diagram is $U_1U_2U_1U_2$, which is equal to U_1U_2 given the relation $U_iU_{i\pm 1}U_i = U_i$.

It can easily be shown that $U_{k_1}U_{k_2}\dots U_{k_\gamma} = U_{k_1}U_{k_2}$ for even values of γ . Our base case is already satisfied. Suppose then that $U_1U_2\dots U_2 = U_1U_2$. Then, $U_1U_2\dots U_2U_1U_2 = (U_1U_2\dots U_2)U_1U_2 = U_1U_2U_1U_2 = U_1U_2$. Proof of the theorem immediately follows from equivalence with U_1U_2 .

The proof for the case where γ is odd is essentially identical to the case where γ is even. □

The next theorem is our final step in generalizing the number of type ii curves formed by diagrams of closures of words in \mathcal{A}_3 of ‘reduced’ form. Specifically, it proves that the number of type ii curves is entirely dependent on the parity of γ , regardless of any exponents on any generators in a word given any arbitrary γ .

Theorem 3.14. *For a word of the form $U_{k_1}^{j_1}U_{k_2}^{j_2}\dots U_{k_\gamma}^{j_\gamma}$, $k_i \neq k_{i+1}$ for all $i = 1, \dots, \gamma - 1$, in \mathcal{A}_3 , if γ is even, then the number of type ii curves in the diagram is equal to 1, and if γ is odd, then the number of type ii curves in the diagram is equal to 2.*

Proof. Consider the case where γ is even. Recall that for even values of γ and $\alpha = \sum_{i=1}^{\gamma} j_i$,

$$\begin{aligned} U_{k_1}^{j_1}U_{k_2}^{j_2}\dots U_{k_\gamma}^{j_\gamma} &= \delta^{\alpha-\gamma}U_{k_1}U_{k_2}\dots U_{k_\gamma} \\ &= \delta^{\alpha-\gamma}U_{k_1}U_{k_2}. \end{aligned} \tag{19}$$

The conclusion for the case where γ is even immediately follows from this equivalence.

Consider the case where γ is odd. Recall that for odd values of γ and $\alpha = \sum_{i=1}^{\gamma} j_i$,

$$\begin{aligned} U_{k_1}^{j_1}U_{k_2}^{j_2}\dots U_{k_\gamma}^{j_\gamma} &= \delta^{\alpha-\gamma}U_{k_1}U_{k_2}\dots U_{k_\gamma} \\ &= \delta^{\alpha-\gamma}U_{k_1}. \end{aligned} \tag{20}$$

The conclusion for the case where γ is odd immediately follows from this equivalence. □

The last theorem of this chapter yields an equation for the total number of curves in a diagram of the closure of any word in \mathcal{A}_3 . Since all curves in such a diagram have been classified as one of two types, the total number of curves in a diagram is the sum of the total number of curves of each type.

Theorem 3.15. *For a word of the form $U_{k_1}^{j_1}U_{k_2}^{j_2}\dots U_{k_\gamma}^{j_\gamma}$, $k_i \neq k_{i+1}$ for all $i = 1, \dots, \gamma - 1$, in \mathcal{A}_3 , the total number of curves in the diagram is equal to $\alpha - \gamma + 2$ if γ is odd, $\alpha - \gamma + 1$ if γ is even.*

Proof. The proof immediately follows from Theorem 3.6 and Theorem 3.14. □

3.3 Generalizations of the Artin Braid Group on Three Strands

The pursuit of a normal form for words in B_3 begins with showing that all words in B_3 are equivalent to another word in B_3 that begins with σ_1 . Theorem 3.16 shows this equivalence to hold given the properties of B_3 as a group.

Theorem 3.16. *Given any braid in B_3 of the form $\sigma_{k_1}^{j_1} \sigma_{k_2}^{j_2} \dots \sigma_{k_\gamma}^{j_\gamma}$, $k_i \neq k_{i+1}$ for all $i = 1, 2, \dots, \gamma - 1$, there exists an equivalent braid in B_3 that begins with σ_1 .*

Proof. For a braid satisfying the hypotheses of the theorem such that the first term is σ_1 , our theorem holds immediately. Recall the relation $\sigma_i \sigma_{i+1} \sigma_i = \sigma_{i+1} \sigma_i \sigma_{i+1}$ for $i = 1, 2, \dots, n - 1$.

$$\begin{aligned} \sigma_2 \sigma_1 \sigma_2 &= \sigma_1 \sigma_2 \sigma_1 \\ \Rightarrow \sigma_2 \sigma_1 &= \sigma_1 \sigma_2 \sigma_1 \sigma_2^{-1} \\ \Rightarrow \sigma_2 &= \sigma_1 \sigma_2 \sigma_1 \sigma_2^{-1} \sigma_1^{-1}. \end{aligned} \tag{21}$$

□

When applying the method given in the proof of theorem 3.16 to a braid beginning with σ_2 , we can note from $\sigma_2^{j_1} \sigma_1^{j_2} \dots \sigma_{k_\gamma}^{j_\gamma} = \sigma_1 \sigma_2 \sigma_1 \sigma_2^{-1} \sigma_1^{-1} \sigma_2^{j_1-1} \sigma_1^{j_2} \dots \sigma_{k_\gamma}^{j_\gamma}$ that the braid word is significantly lengthened. Since the aim of these proofs is to simplify the calculation of invariants from braid words, it would be desirable to reduce equivalent braids to their shortest possible form. This can be achieved by a weaker theorem that allows for the consideration of equivalence of braid closures, thus giving us access to Markov's theorem. It is clear that the first two moves in Markov's Theorem satisfy the axioms of an equivalence relation.

Theorem 3.17. *Given any braid in B_3 of the form $\sigma_{k_1}^{j_1} \sigma_{k_2}^{j_2} \dots \sigma_{k_\gamma}^{j_\gamma}$, $k_i \neq k_{i+1}$ for all $i = 1, 2, \dots, \gamma - 1$, there exists a braid in B_3 with an equivalent closure that begins with σ_1 .*

Proof. Consider $\sigma_{k_1}^{j_1} \sigma_{k_2}^{j_2} \dots \sigma_{k_\gamma}^{j_\gamma}$. In the case where $k_1 = 1$, our theorem holds immediately.

Suppose $k_1 = 2$. Consider the case where γ is even. Then, $\sigma_{k_\gamma}^{j_\gamma} = \sigma_1^{j_\gamma}$, and thus

$$\sigma_{k_1}^{j_1} \sigma_{k_2}^{j_2} \dots \sigma_{k_\gamma}^{j_\gamma} = \sigma_2^{j_1} \sigma_1^{j_2} \dots \sigma_1^{j_\gamma}.$$

$$\begin{aligned} \sigma_2^{j_1} \sigma_1^{j_2} \dots \sigma_1^{j_\gamma} &\equiv_c \sigma_1^{j_\gamma} \sigma_2^{j_1} \sigma_1^{j_2} \dots \sigma_1^{j_\gamma} \sigma_1^{-j_\gamma} \\ &= \sigma_1^{j_\gamma} \sigma_2^{j_1} \sigma_1^{j_2} \dots \sigma_2^{j_{\gamma-1}}. \end{aligned} \tag{22}$$

Consider the case where γ is odd. Then, $\sigma_{k_\gamma}^{j_\gamma} = \sigma_2^{j_\gamma}$, and thus $\sigma_{k_1}^{j_1} \sigma_{k_2}^{j_2} \dots \sigma_{k_\gamma}^{j_\gamma} = \sigma_2^{j_1} \sigma_1^{j_2} \dots \sigma_2^{j_\gamma}$.

$$\begin{aligned} \sigma_2^{j_1} \sigma_1^{j_2} \dots \sigma_2^{j_\gamma} &\equiv_c \sigma_2^{-j_1} \sigma_2^{j_1} \sigma_1^{j_2} \dots \sigma_2^{j_\gamma} \sigma_2^{j_1} \\ &= \sigma_1^{j_2} \sigma_2^{j_3} \dots \sigma_2^{j_\gamma + j_1}. \end{aligned} \tag{23}$$

□

The last theorem in this chapter establishes that, for all words in B_3 of length greater than one, the diagram of the closure of such a word is equivalent under ambient isotopy to some word of even length. The restriction to equivalence of diagrams of the closures of words allows access to Markov's Theorem once again, and thus equivalence under conjugation.

Theorem 3.18. *Given any braid in B_3 of the form $\sigma_{k_1}^{j_1} \sigma_{k_2}^{j_2} \dots \sigma_{k_\gamma}^{j_\gamma}$, $k_i \neq k_{i+1}$ for all $i = 1, 2, \dots, \gamma - 1$, $\gamma > 1$, there exists another braid in B_3 with an equivalent closure such that γ is even.*

Proof. From theorem 3.17, we can consider without loss of generality a braid word of the form $\sigma_1^{j_1} \sigma_2^{j_2} \dots \sigma_{k_\gamma}^{j_\gamma}$. If γ is even, our theorem immediately holds. Consider the case where γ is odd. Then $\sigma_{k_\gamma} = \sigma_1$, and $\gamma - 1$ is even.

$$\begin{aligned} \sigma_1^{j_1} \sigma_2^{j_2} \dots \sigma_1^{j_\gamma} &\equiv_c \sigma_1^{j_\gamma} \sigma_1^{j_1} \sigma_2^{j_2} \dots \sigma_1^{j_\gamma} \sigma_1^{-j_\gamma} \\ &= \sigma_1^{j_1+j_\gamma} \sigma_2^{j_2} \dots \sigma_2^{j_{\gamma-1}}. \end{aligned} \tag{24}$$

□

4 FURTHER RESEARCH

There are two desirable properties that we would like to have in a normal form for the Artin braid group and the Temperley-Lieb Algebra. First, we would like for our normal form to have a one-to-one correspondence between a braid's normal form and the Jones polynomial associated with the link formed by the braid's closed diagram. Second, we would like our normal form to be applicable for an arbitrary number of strands n in both the Artin braid group and the Temperley-Lieb algebra. Further work is needed to extend the theorems in this thesis to generalizations that apply for an arbitrary number of strands n , and more theorems not yet begun in the case of 3 strands may be necessary in order for our normal form to have these two desirable properties.

BIBLIOGRAPHY

- [1] *Knots and Physics*, 3rd edition, by Louis H. Kauffman, Published by World Scientific Publishing Co. Pte. Ltd. 1993.
- [2] *Introduction to Knot Theory*, edition, by Richard H. Crowell and Ralph H. Fox, Publised by Ginn 1963.
- [3] *An Introduction to Knot Theory*, edition, by William B. Lickorish, Published by Springer 1997.
- [4] *Topology*, 2nd edition, by James Munkres, Published by Pearson Education 2000.
- [5] *Knot Theory and Its Applications*, edition, by Kunio Murasugi, Published by Birkhauser 2008.

APPENDIX: PYTHON CODE IMPLEMENTATION

The python code that follows computes the Jones polynomial given a braid word in the form of a list, where the list is a sequence of generators and their inverses raised to a single power. Theorem 3.15 is implemented in the ‘state_value’ function.

```
from sympy import *  
  
from sympy.abc import sigma, delta  
  
u1 = Symbol('U_1', commutative = False)  
u2 = Symbol('U_1', commutative = False)  
sigma_1 = Symbol('sigma_1', commutative = False)  
sigma_2 = Symbol('sigma_2', commutative = False)  
A = Symbol('A')  
t = Symbol('t')  
sigma1 = (A + A**(-1) * u1)  
sigma2 = (A + A**(-1) * u2)  
sigma1_inverse = (A**(-1) + A * u1)  
sigma2_inverse = (A**(-1) + A * u2)  
  
def calculate_writhe(braid_word_array):  
    if type(braid_word_array) != list:
```

```

        sigma_list = str(braid_word_array)
else:
    sigma_list = ''.join(str(e) for e in braid_word_array)
total_sigma = sigma_list.count('sigma')
total_negative = sigma_list.count('-1')
total_positive = total_sigma - total_negative
return total_positive - total_negative

def rho(factor):
    if factor == sigma_1:
        return sigma1
    elif factor == sigma_1**(-1):
        return sigma1_inverse
    elif factor == sigma_2:
        return sigma2
    elif factor == sigma_2**(-1):
        return sigma2_inverse

def rho_map(braid_word_array):
    tl_sum = 1
    # single factor braids are not read as lists,

```

```

# thus this simplified parsing is implemented in this case
if type(braid_word_array) != list:
    tl_sum *= rho(braid_word_array)
else:
    for factor in braid_word_array:
        tl_sum *= rho(factor)
return tl_sum

def reduced_length(factor):
    return factor.count(u1) + factor.count(u2)

def state_value(factor):
    # State value for the identity is delta squared
    if reduced_length(factor) == 0:
        return factor * delta**2
    # From Theorem 3.15, products of even reduced length
    # evaluate to delta raised to a power equal to the
    # exponent sum minus the reduced length.
    # Exponent sum is calculated by substituting all
    #  $U_n^{**k}$  with  $\text{delta}^{**k}$ , where  $k$  gives the exponent sum.

```

```

# Length is subtracted by dividing by delta**m,
# where m is the reduced length.

elif (reduced_length(factor) % 2) == 0:
    newarg = factor.subs(u1, delta).subs(u2, delta)
    return newarg * delta**(-reduced_length(factor))
# From Theorem 3.15, products of odd reduced length
# evaluate to delta raised to a power equal to the
# exponent sum minus the reduced length, plus one.
else :
    newarg = factor.subs(u1, delta).subs(u2, delta)
    return newarg * delta**(-reduced_length(factor) + 1)

def bracket(polynomial):
    output = 0
    for arg in polynomial.args:
        output += state_value(arg)
    return output

def normalize_by_writhe(writhe):
    return (-A**3)**(-1 * writhe)

```

```

def jones (polynomial):
    tl_sum = expand(rho_map(polynomial))
    writhe = calculate_writhe(polynomial)
    jones = simplify(normalize_by_writhe(writhe) *
        bracket(tl_sum).subs(delta, -(A**2) -
            A**(-2))).subs(A, t**(-1/4))
    return simplify(jones)

# input must be in the form of an array, factor by factor
# example: [sigma_1, sigma_2, sigma_1, sigma_2**(-1), sigma_1**(-1),
# sigma_1**(-1), sigma_1], which will return the jones polynomial
# for the Hopf-Link, -t**(-0.5) - t**(0.5)

```

VITA

JACK HARTSELL

Education: B.S. Physics, East Tennessee State University,
Johnson City, Tennessee 2013
M.Sc. Mathematical Sciences, East Tennessee
University, Johnson City, Tennessee 2018

Professional Experience: Graduate Assistant, Instructor, East Tennessee State
University, Johnson City, Tennessee, 2016–2018